Stanford Exploration Project, Report 103, April 27, 2000, pages 123–149

Variable-velocity prestack Stolt residual migration with application to a North Sea dataset

Paul Sava[1]

ABSTRACT

This paper investigates the applicability of prestack Stolt residual migration when the original image is obtained using an arbitrary velocity model. At its origin, the method is based on an assumption of constant velocity. However, its formulation for depth-migrated images involves a ratio of the reference and target velocities; therefore, for residual migration it is completely irrelevant if the original migration uses constant or variable velocity. Several examples, both on synthetic and real data demonstrate the effectiveness of the method. When applied to a North Sea dataset, the method highlights important features not seen in the original migration.

INTRODUCTION

Prestack Stolt residual migration has recently gained a new momentum because of its usefulness in imaging and migration velocity analysis (Biondi and Sava, 1999; Sava and Biondi, 2000). The method's main merit is that instead of requiring an assumption about the magnitude of the target velocity model to which we want to residually migrate, it only calls for an assumption about the ratio of the reference velocity to the target velocity (Sava, 1999b,a). Since the method is, in essence, a Stolt-stretch technique, it inherits Stolt's speed and convenience.

As for other Stolt-type techniques, the derivation of the method is based on the assumption of constant velocity. However, if we start from a depth-migrated image, the residual migration process can be shown not to depend on the actual velocities anymore, but rather on the ratio of the reference (v_0) and correct (v) velocities.

Strictly speaking, the ratio corresponds to two constant velocities. This would imply, however, that we obtain the original image using constant velocity as well, which is normally not the case. In this paper, I investigate the applicability of the residual migration method to images obtained using variable velocity models. I begin with a brief review of the theory and continue with three synthetic examples and one real-data example, which demonstrate that, although not theoretically accurate, the method can still be used in cases of variable velocity media.

[1]**email:** paul@sep.stanford.edu

THEORY REVIEW

Stolt residual migration is formulated both for post-stack and prestack data. Stolt (1996) shows that, for the post-stack case, the residual migration operator is a function of the difference between the squared values of the original velocity and the new velocity to which the image is residually migrated. However, Stolt shows that such a formulation is no longer possible in the prestack case.

Sava (1999b,a) reformulates Stolt residual migration for depth-migrated images and shows that the operator is a function of the ratio of the two velocities, before and after residual migration, a formulation that holds for both post-stack and prestack (2-D, 3-D and common-azimuth) data.

In the 3-D case, the residual migration equation takes the form

$$k_z = \frac{1}{2}\sqrt{\frac{v_0^2}{v^2}\frac{\left[4k_{z_0}^2+\left(\left|\vec{k}_m+\vec{k}_h\right|-\left|\vec{k}_m-\vec{k}_h\right|\right)^2\right]\left[4k_{z_0}^2+\left(\left|\vec{k}_m+\vec{k}_h\right|+\left|\vec{k}_m-\vec{k}_h\right|\right)^2\right]}{16k_{z_0}^2}-\left|\vec{k}_m-\vec{k}_h\right|^2} + \frac{1}{2}\sqrt{\frac{v_0^2}{v^2}\frac{\left[4k_{z_0}^2+\left(\left|\vec{k}_m+\vec{k}_h\right|-\left|\vec{k}_m-\vec{k}_h\right|\right)^2\right]\left[4k_{z_0}^2+\left(\left|\vec{k}_m+\vec{k}_h\right|+\left|\vec{k}_m-\vec{k}_h\right|\right)^2\right]}{16k_{z_0}^2}-\left|\vec{k}_m+\vec{k}_h\right|^2}, \tag{1}$$

where

- k_{z0} and k_z are depth wavenumbers before and after residual migration,
- v_0 and v are, respectively, the reference and the target migration velocities, and
- $\vec{k}_m$ and $\vec{k}_h$ are the offset and midpoint wavenumbers.

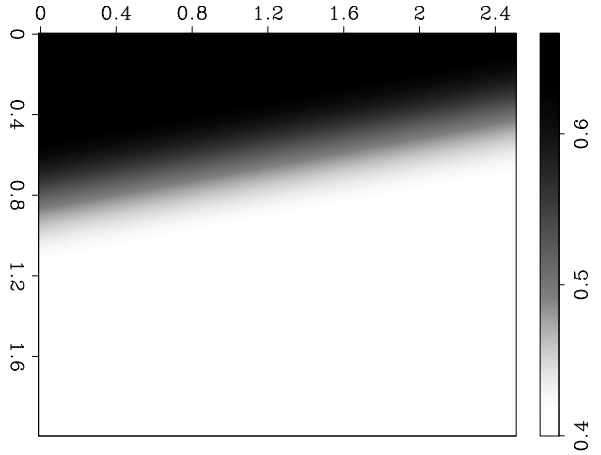

Figure 1: The slowness map used for the first 2-D synthetic examples. paul1-dipsynt.slo [CR]

Strictly speaking, Equation (1) is derived from the constant velocity dispersion relations for pre-stack data. However, since the new images do not depend on the true magnitude of the new velocity, but rather on its ratio to the original, we can still techniquely apply residual migration, even when the original velocity is variable. The question is how valid such a residual migration operation is for the case of variable velocity, and whether the output provides

any valuable information. A theoretical answer is not straightforward, since most likely the answer is data-dependent. I will, therefore, address the problem in an experimental way, first on synthetic models, and then on a North Sea real dataset.

SYNTHETIC EXAMPLES

I begin with two simple synthetic models. The first consists of a succession of flat reflectors embedded in a variable velocity model (Figure 1).

The left panel of Figure 2 shows the result of migration with the correct velocity, while the middle panel shows the result of migration with a scaled version of the original, and the right panel shows the result of residual migration using the correct velocity ratio. The flat reflectors are all restored to their original position, and the angle-domain common-image gathers are flat, indicating correct migration.

Figure 3 depicts a more complex model. In this case, the reflectors have different dips, and the velocity is variable and identical to the one in the preceding case (Figure 1). Again, the left panel shows the migration result with the correct velocity, the middle panel the result of migration with an incorrect velocity, and the right panel the result of residual migration with the correct velocity ratio. The reflectors are restored to their correct position and the angle-domain common-image gathers are flat.

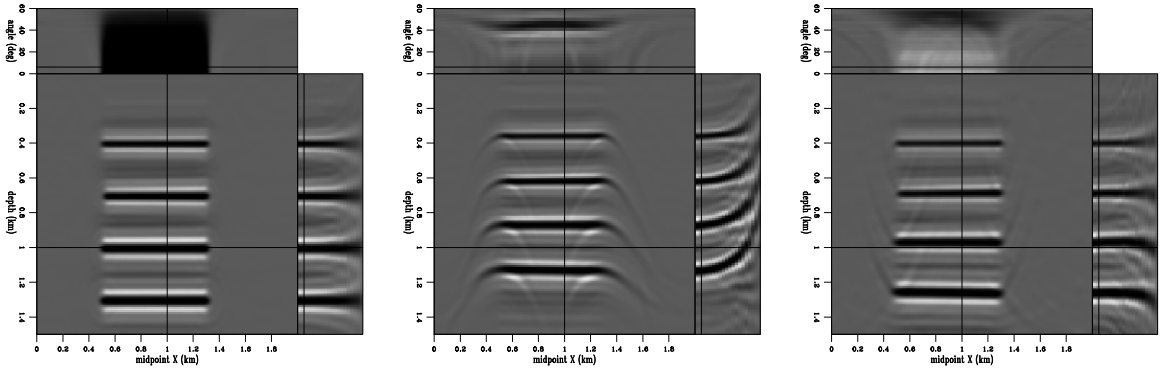

Figure 2: A simple synthetic model made of flat reflectors. The left panel represents migration with the correct velocity. The middle panel represents migration with an incorrect velocity, and the right panel represents the result of residual migration applied to the image in the middle panel. The reflectors are restored very close to their correct position. paul1-flatsynt.cig [CR]

The next synthetic example is represented by an image around a salt body. As in the preceding examples, the left panel of Figure 4 shows the result of migration with the correct velocity, in the middle panel the result of migration with an incorrect velocity, and in the right panel, the result of residual migration with the correct velocity ratio. Again, we can conclude that prestack Stolt residual migration is able to recover the correct image, even when the velocity map is not constant. We can, therefore, apply the procedure to a much more complex seismic image obtained from data recorded over a North Sea salt dome.

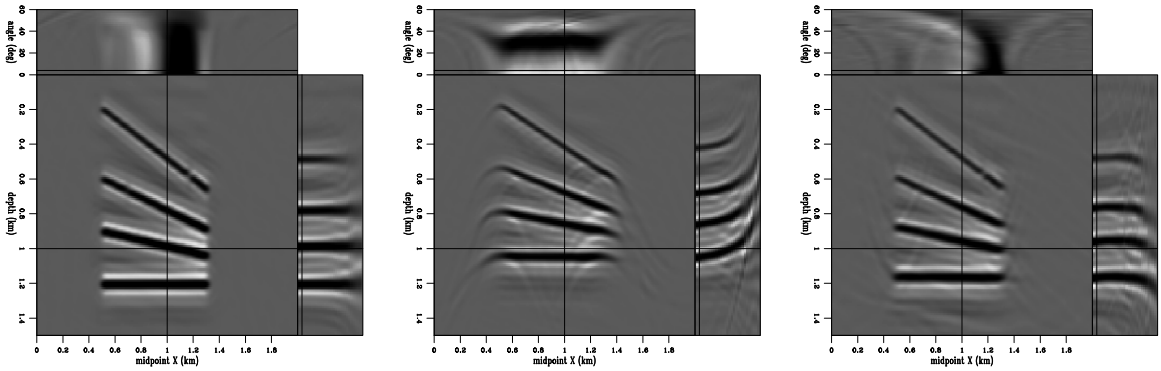

Figure 3: A simple synthetic model made of dipping reflectors. The left panel represents migration with the correct velocity. The middle panel represents migration with an incorrect velocity, and the right panel represents the result of residual migration applied to the image in the middle panel. The reflectors are restored very close to their correct position. paul1-dipsynt.cig [CR]

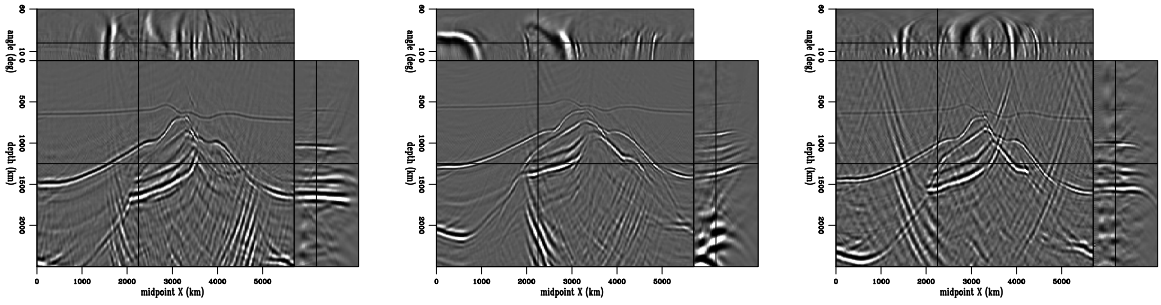

Figure 4: A complex synthetic model around a salt body. The left panel represents migration with the correct velocity. The middle panel represents migration with an incorrect velocity, and the right panel represents the result of residual migration applied to the image in the middle panel. The reflectors are restored to their correct position. paul1-saltsynt.cig [CR]

A NORTH SEA EXAMPLE

The North Sea dataset used in this paper has been previously discussed by Vaillant and Sava (1999). Figure 5 shows a 2-D slice out of the image-cube obtained by common-azimuth migration (Biondi and Palacharla, 1996). Without going into many details, we can observe that many of the important features of the image have been well resolved, especially away from the salt. However, there still are some regions in the image insufficiently clarified, as labeled in Figure 5:

1. (**A**) Where is the salt overhang flank?
2. (**B**) How do the sediments terminate against the salt?
3. (**C**)(**D**) What is this?

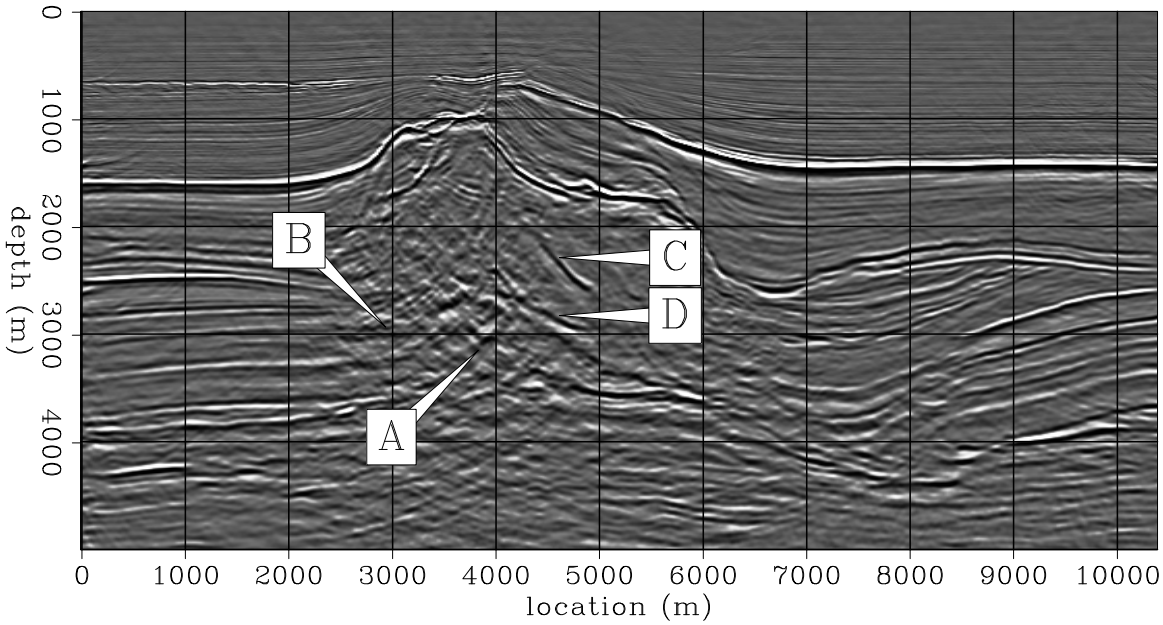

Figure 5: Seismic image for the North Sea data. Major questions still unanswered are A Where is the salt overhang flank? B How do the sediments terminate against the salt? C D What is this? paul1-saltreal.problem [CR]

Essentially, an important area of the image, close to the overhang, remains under severe blur caused by the salt body. This area, encircled with question marks in Figure 6, is the focus for the residual migration processing. Two hypotheses can be made about the cause of the blur:

- it is caused by inaccuracies of the imaging algorithm, a hypothesis that is analyzed elsewhere (Vaillant and Calandra, 2000);

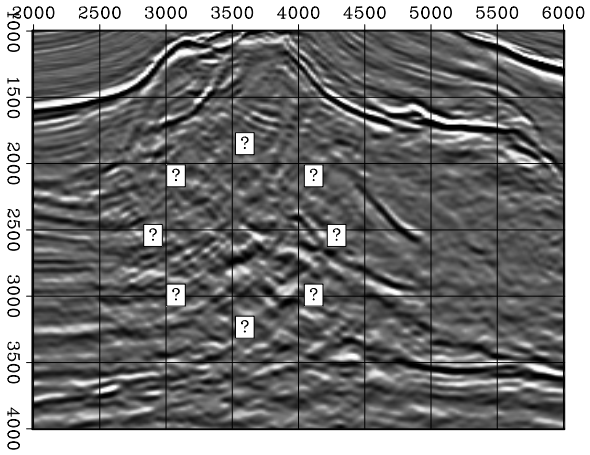

Figure 6: Zoom over the area of major blur. The goal of the residual migration is to shed as much light as possible over the region encircled with question marks. paul1-saltreal.zoom [CR]

- the velocity map around the salt body is not correct, a hypothesis which is the focus of this paper.

Since in this case we are analyzing a real dataset, we do not know what the correct velocity ratio ($\gamma = \frac{v_0}{v}$) is to which we would like to residually migrate. Most likely, in fact, there is no one velocity ratio that would solve the problem over the entire seismic image. What we need to do then is run residual migration for a range of velocity ratios and analyze what changes have occurred. In the end, we should either select one image which answers our questions, or interpolate an optimal image.

Figure 7 shows how the target image is changed when the parameter γ varies from 0.90 to 1.00. A value of $\gamma < 1.0$ indicates that we residually migrate the image with a *higher velocity* than the original. It is apparent that the overhang salt flank is significantly better imaged at higher velocities compared to the reference image. Also, many of the layers in the image continue under the salt, and therefore become much easier to interpret.

Figure 8 represents a face-to-face comparison of the original image (left panel) and a cleaner image obtained with residual migration (right panel), which enables us to answer some of the questions posed at the beginning of the discussion:

1. The salt flank (**F**) is more continuous and extends significantly more towards the surface. It is also more energetic, and positioned lower in the image. Since this reflector is imaged mostly with the salt velocity, we can conclude that the salt velocity is not high enough in the original model and therefore needs to be increased to achieve better imaging.

2. The reflector (**R**), previously imaged inside the salt, appears much fainter, perhaps simply indicating that this event is merely an artifact or a salt internal multiple.

3. The sediments below the salt **S** are significantly cleaner. What is practically not interpretable in the original image becomes much cleaner and makes a lot more geological sense. We can, in fact, trace how the sediments bend against the salt body.

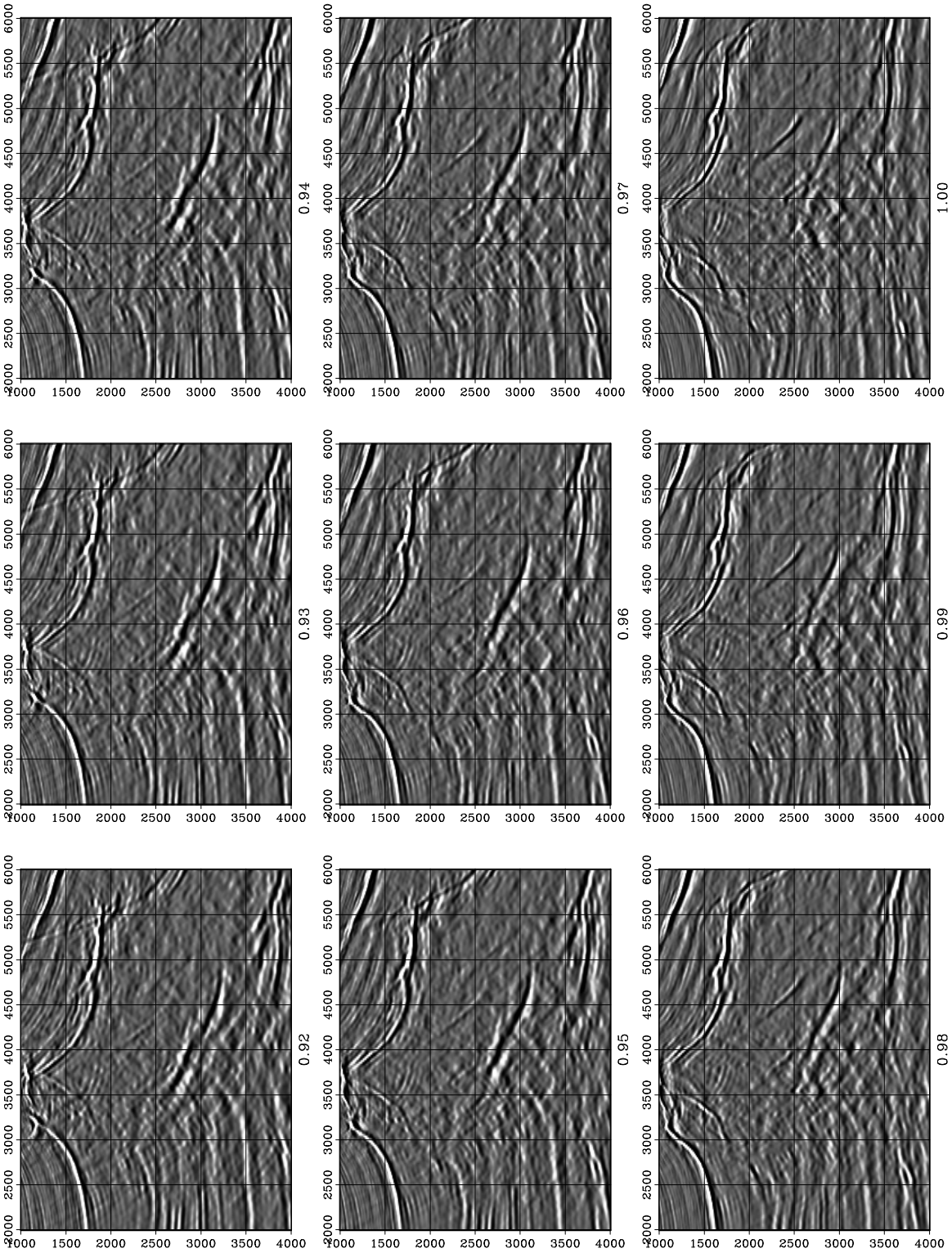

Figure 7: Residual migration results. Each panel represent the image corresponding to different values of the parameter γ, ranging from 0.92 to 1.00. The salt flank is significantly better imaged at lower values of γ, that is, at velocity values higher than those of the original model. paul1-saltreal.storm [CR]

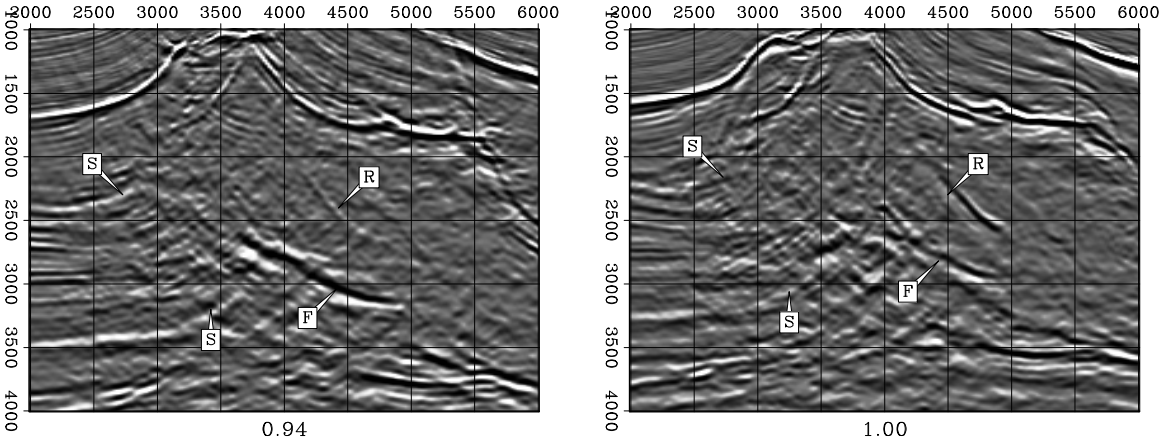

Figure 8: A face-to-face comparison of the original seismic image (left) and an image obtained by residual migration with the ratio $\gamma = 0.94$ (right). paul1-saltreal.face2face [CR]

The downside of selecting only an image corresponding to a constant parameter γ over the entire map is that the image degrades in the regions that do not require an increase in velocity, or that may only require a smaller increase. A good example is the upper part of the salt, which appears slightly over-migrated and defocused in the residual migration panel (Figure 8, left) with respect to the original image (Figure 8, right).

A reasonable solution to this problem is to pick different ratios at every location in the images in Figure 7. The interpolation aim is to preserve the original image in the regions where it is correct and to bring into the picture the regions that show improvement after residual migration. Figure 9 shows the result of optimal picking:

- The top part of the salt, between the horizontal locations 2500 and 3500 m, where the remaining diffraction in the original image is much better collapsed at a higher velocity ($\gamma = 0.97$).
- The overhang salt flank and the sediments underneath are much cleaner after residual migration than in the original. This situation also corresponds to a higher velocity ($\gamma = 0.94$).

CONCLUSIONS

This paper shows that prestack Stolt residual migration, in spite of its constant velocity origin, can be successfully applied to depth images obtained with an arbitrary velocity. Several examples, both on synthetic and on real data, prove the effectiveness of the method. The key to improving the seismic images lies in correctly picking the variable surface of the parameter γ, rather than in selecting only one image at a particular value.

The method also shows that the blurred regions of the seismic image of the North Sea dataset are not so much an imaging problem as a velocity problem: a better velocity map

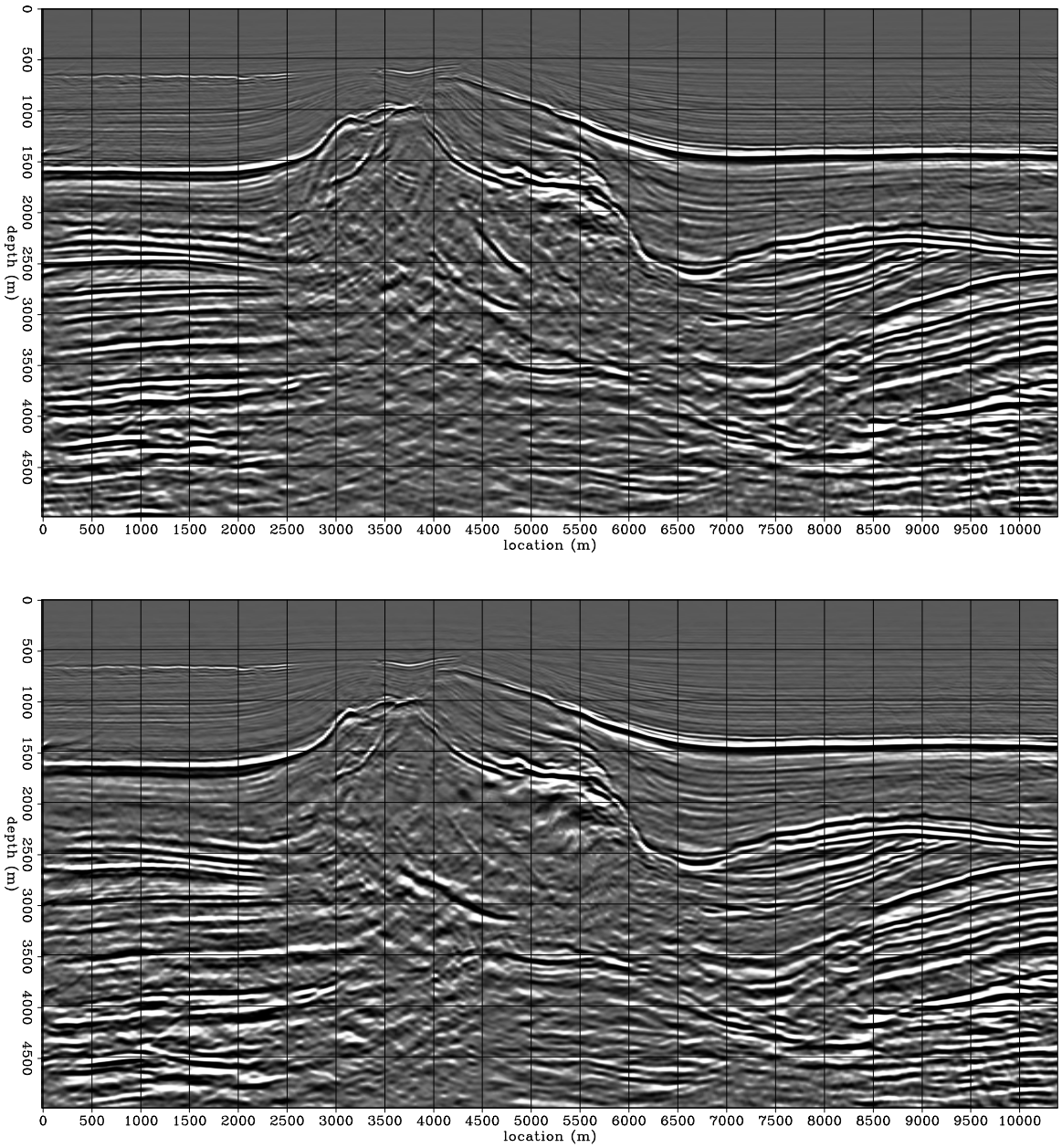

Figure 9: Comparison between the images before and after residual migration. The top panel is the image obtained with common-azimuth migration on the original velocity model. It shows incomplete focusing in the upper part of the salt and blurred salt overhang. The bottom panel is the image after residual migration, and shows a collapsed diffraction at the top of the salt, and much better imaged salt overhang and under-salt sediments. paul1-saltreal.comparison [CR]

could enable a good algorithm to image the overhang of the salt, at least partially. Prestack Stolt residual migration is able to improve the migrated image, at a fraction of the cost of the original migration.

ACKNOWLEDGMENTS

I would like to thank Biondo Biondi for many stimulating discussions. Elf Aquitaine provided both the synthetic salt-dome model and the North Sea dataset.

REFERENCES

Biondi, B., and Palacharla, G., 1996, 3-D prestack migration of common-azimuth data: Geophysics, **61**, no. 6, 1822–1832.

Biondi, B., and Sava, P., 1999, Wave-equation migration velocity analysis: SEP–**100**, 11–34.

Sava, P., and Biondi, B., 2000, Wave-equation migration velocity analysis: Episode II: SEP–**103**, 19–47.

Sava, P., 1999a, Short note–on Stolt common-azimuth residual migration: SEP–**102**, 61–66.

Sava, P., 1999b, Short note–on Stolt prestack residual migration: SEP–**100**, 151–158.

Stolt, R. H., 1996, Short note–a prestack residual time migration operator: Geophysics, **61**, no. 2, 605–607.

Vaillant, L., and Calandra, H., 2000, Common-azimuth migration and Kirchhoff migration for 3-D prestack imaging: A comparison on North Sea data: SEP–**103**, 139–147.

Vaillant, L., and Sava, P., 1999, Common-azimuth migration of a North Sea dataset: SEP–**102**, 1–14.